



Synthesis and performance study of zinc borate nanowhiskers

Yunhui Zheng^a, Yumei Tian^{a,*}, Honglei Ma^b, Yuning Qu^a, Zichen Wang^a, Dongmin An^a, Shuang Guan^a, Xiaoyan Gao^a

^a College of Chemistry, Jilin University, Changchun, 130012, China

^b Changchun Institute of Optics, Fine Mechanics and Physics, Chinese Academy of Sciences, Changchun, 13000, China

ARTICLE INFO

Article history:

Received 6 December 2008

Received in revised form 10 February 2009

Accepted 12 February 2009

Available online 23 February 2009

Keywords:

Zinc borate

Nanowhiskers

Chemical synthesis

Crystal structure

ABSTRACT

Zinc borate ($4\text{ZnO} \cdot \text{B}_2\text{O}_3 \cdot \text{H}_2\text{O}$) nanowhiskers were synthesized via one-step precipitation reaction in aqueous solution of sodium borate ($\text{Na}_2\text{B}_4\text{O}_7 \cdot 10\text{H}_2\text{O}$) and zinc nitrate ($\text{Zn}(\text{NO}_3)_2 \cdot 6\text{H}_2\text{O}$) with phosphate ester as the modifying agent. The zinc borate nanowhiskers have the monoclinic crystal structure with diameters of 50–100 nm, lengths of about 1 μm , and the aspect ratios close to 10–20. Finally the thermal stability of polyethylene has been shown to increase upon the addition of the nanowhiskers to it.

© 2009 Elsevier B.V. All rights reserved.

1. Introduction

During the past decade there has been a growing interest in synthesizing whiskers as nanoreinforcement in polymer matrixes [1–3]. The reinforced ability of the whiskers lies in their high surface area and good mechanical properties [4–9]. The incorporation of nanomaterials such as layered silicate clays, calcium carbonate or other nanoparticles arranged on the nanometer scale with a high aspect ratio and/or an extremely large surface area into polymers improves significantly their mechanical performances. Combination of characteristics such as light-weight, corrosion resistance, low to moderate cost, thermal stability and easy processability, make them attractive for many applications especially in automotive industry [10–12].

The uniform dispersion of nanofillers in the polymer matrixes is a general prerequisite for achieving desired mechanical and physical characteristics. So the surface modification techniques had been developed to improve the physical and chemical properties of the nanosurfaces, with small organic molecules or polymers. It was also found that the presence of chemical bonds between the nanofillers and polymer matrixes could improve greatly the thermal and mechanical properties of the polymer nanocomposites [13–15].

Various processes have been explored to synthesize nanowhiskers [16]. The preparation of the whiskers, however, is still one of the biggest challenges in chemistry and materials

science. For the past few years, different methodologies have been developed for the preparation of nanowhiskers. Park et al. synthesized single-crystalline cubic barium titanate (BaTiO_3) whiskers through sol–gel reactions of bimetallic precursors ($\text{BaTi}(\text{O}_2\text{CCH}_3)_6$), in a hot organic solvent initiated by injection of aqueous H_2O_2 solution [17]. Until now, there have been still no literature reports about synthesis of hydrophobic zinc borate whiskers via one-step precipitation reaction.

In the course of our investigation of borate nanomaterials, we have unexpectedly obtained hydrophobic zinc borate whiskers, which require neither sophisticated techniques nor catalysts. The higher aspect ratio products are successfully prepared through this method. The hydrophobic products can be easily combined with the polymer and showed the better thermal stabilities.

2. Experimental

2.1. Materials

All chemicals used in the synthetic procedures of this work were purchased from Beijing Chemicals Co. Ltd., which were of analytical purity and without any further treatments. Distilled water was applied for all synthesis and treatment processes.

2.2. Methods

In a typical procedure, 50 mL of 0.1 mol dm^{-3} $\text{Na}_2\text{B}_4\text{O}_7 \cdot 10\text{H}_2\text{O}$ aqueous solution and 1 mL of 0.002 mol dm^{-3} phosphate ester were loaded into a 250-mL three-neck round-bottom flask equipped with

* Corresponding author. Tel.: +86 431 85155358; fax: +86 431 85155358.
E-mail address: tianym@jlu.edu.cn (Y. Tian).

a thermometer and a mechanical stirrer. The mixture was heated to 70 °C, to which 10.0 mL of 2 mol dm⁻³ Zn(NO₃)₂·6H₂O aqueous solution was added over 0.5 h while being stirred [18,19]. The reaction (pH 8.0) was then continued at the same temperature for about 7 h. The precipitate was collected and washed several times with absolute ethanol and distilled water to remove the by-products, and then dried at 60 °C for 8 h to obtain the final white zinc borate powders.

Afterwards, 10 g polyethylene (PE) was dissolved in the solvent of 50 mL cyclohexane in another 250 mL three-neck round-bottom flask equipped with a mechanical stirrer. A certain amount of synthesized products were then added to the dissolved PE over 1 h. The mixture was finally poured on a piece of clean glass to form a film.

2.3. Characterizations

The structure and composition of products were analyzed by X-ray powder diffraction (XRD) (SHIMADZU XRD-6000 diffractometer employing Ni-filtered Cu K α radiation, at a scanning rate of 6°/min with 2 θ ranging from 15° to 50°).

The morphology and the size of the samples were examined using a Hitachi scanning electron microscope (SEM) with a field-emission-scanning electron microscope (JEOL-6700F) and a Hitachi H-800 transmission electron microscope (TEM), at an accelerator voltage of 200 kV. The powders were dispersed in absolute ethanol and ultrasonicated before SEM and TEM characterization.

Water contact angle of sample was measured by using a FT Λ 200 (USA) contact angle analyzer. IR spectroscopy of the samples as powder-pressed KBr pellets were examined in the wave number range from 4000 to 500 cm⁻¹ at a resolution of 4 cm⁻¹ using a JIR-5500 (JEOL) spectrophotometer at room temperature. Thermogravimetric analysis (TGA) was carried out using a DTG-60H analyzer (SHIMADZU).

3. Results and discussion

3.1. X-ray diffraction diagrams of zinc borate

The synthesized product is stable white powder at room temperature. The XRD patterns of the as-synthesized samples can be perfectly indexed to the pure phase of the monoclinic crystal structure of 4ZnO·B₂O₃·H₂O [20,21].

The temperature was of great effect to the reaction as indicated by the increased relative intensity of the XRD diffraction peaks with increased temperature. The products had not been well crystallized when the reaction temperatures were 30 °C (Fig. 1a) and 50 °C (Fig. 1b). The crystallization of 4ZnO·B₂O₃·H₂O was significantly improved when the reaction temperature was increased to 70 °C (Fig. 1c). This was due to the rate of reaction being enhanced when the reaction temperature was elevated.

3.2. TGA of the powders

To investigate as to whether the reaction products were the configuration of 4ZnO·B₂O₃·H₂O crystals, the products obtained were tested by TGA. Fig. 2 shows TGA thermograms of weight as a function of temperature for modified zinc borate (Fig. 2a) and phosphate ester (Fig. 2b) with a heating rate of 20 °C min⁻¹ in the temperature range from 50 to 900 °C.

The initial weight loss for all the samples occurred at 100–200 °C due to the moisture evaporation and the second part of the weight loss was phosphate ester decomposing when the temperature was at 200–400 °C, which could be showed in Fig. 2b. The major weight losses were in the range of 400–600 °C for modified zinc borate, which might be correspondent to the crystal water.

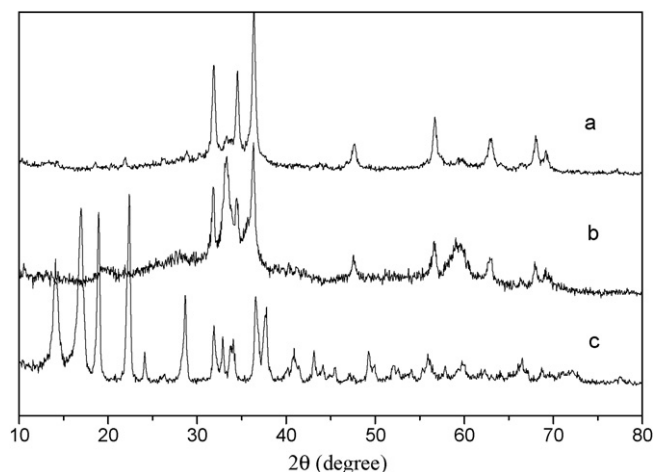


Fig. 1. XRD of products obtained at pH 8: (a) 30 °C; (b) 50 °C; (c) 70 °C for 7 h with phosphate ester.

Fig. 2a curve indicates that the weight loss was 4.44% from 400 to 600 °C, which corresponded to the loss of one molar equivalent of the crystal water and could be compared with calculated value of 4.45% and formed 4ZnO·B₂O₃·H₂O. The TGA result was consistent with the XRD result.

3.3. SEM micrograph of the powders

Fig. 3 shows a set of typical SEM images corresponding to the samples obtained from the solution with pH 8.0 at different reaction temperatures for 7 h. They were controlled by phosphate ester except Fig. 3a. The products were irregular in Fig. 3a and b, which were made at 70 °C without phosphate ester and at 30 °C with phosphate ester, respectively. When the reaction temperature was increased to 50 °C, a few zinc borate nanowhiskers were formed (Fig. 3c), and the whiskers were the major product as the reaction temperature was increased to 60 °C (Fig. 3d). When the temperature reached 70 °C, 4ZnO·B₂O₃·H₂O nanowhiskers were the only product with 50–100 nm in diameter, about 1 μ m in length, and 10–20 in the aspect (Fig. 3e). As will be discussed in the following section, the products obtained through this method could be well dispersed into polyethylene (PE).

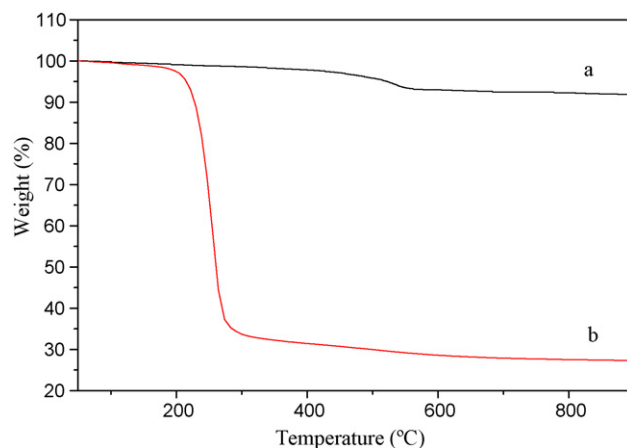


Fig. 2. TGA of: (a) the hydrophobic zinc borate (h-ZB) obtained at pH 8 and 70 °C for 7 h with phosphate ester and (b) pure phosphate ester.

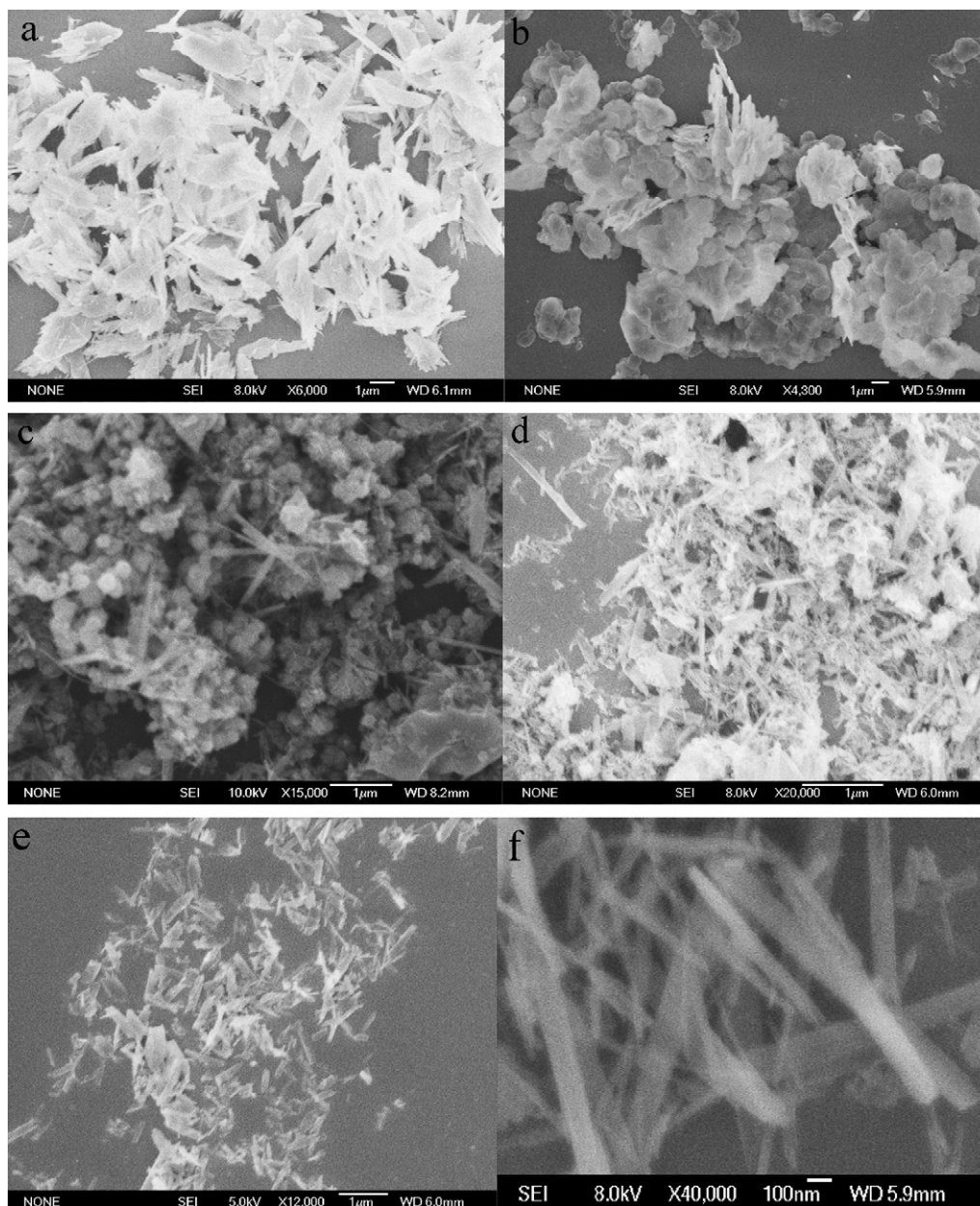


Fig. 3. SEM images of samples prepared at pH 8 for 7 h: (a) at 70 °C without phosphate ester; (b) at 30 °C with phosphate ester; (c) at 50 °C with phosphate ester; (d) at 60 °C with phosphate ester; (e) low magnification at 70 °C with phosphate ester; (f) high magnification at 70 °C with phosphate ester.

3.4. TEM micrograph of the products

Fig. 4 shows the internal framework of low-magnification image (Fig. 4a) and high-magnification image (Fig. 4b) of the hydrophobic zinc borate (h-ZB), respectively, which proved the results of the SEM either. The lattice in an electron diffraction pattern appeared due to the diffracted electron beam from a set of lattice planes in the crystallites present in the sample satisfying the Bragg diffraction condition. Using this selected-area electron diffraction (SAED) technique, hydrophobic zinc borate nanowhiskers were revealed to be perfectly single-crystalline and grew along the [0 0 2] and [2 3 0] directions (inset in Fig. 4b).

3.5. Contact angle of the hydrophobic zinc borate

The contact water angle was widely used as a criterion for evaluating surface hydrophobicity. In order to study the surface

characteristics, the zinc borate powder was analyzed to measure the relative contact angle. Fig. 5 presents the changes of the contact angle containing the unmodified products (without added phosphate ester) and the modified products (with added phosphate ester) from the low synthetic temperature to the high synthetic temperature. The pure products had the smallest contact angle (Fig. 5d). When the synthesis temperature was enhanced from 30 to 70 °C (Fig. 5a–c), the wettability of products was decreased. The biggest contact angle was 115.26° when the whiskers were synthesized at 70 °C for 7 h. From the results, we could deduce that the contact angle was increased while the synthesis temperature was increased.

3.6. FT-IR spectrum of the composite nanowhiskers

FT-IR was used to determine which functional groups are presented in the samples. Fig. 6 shows that the products without

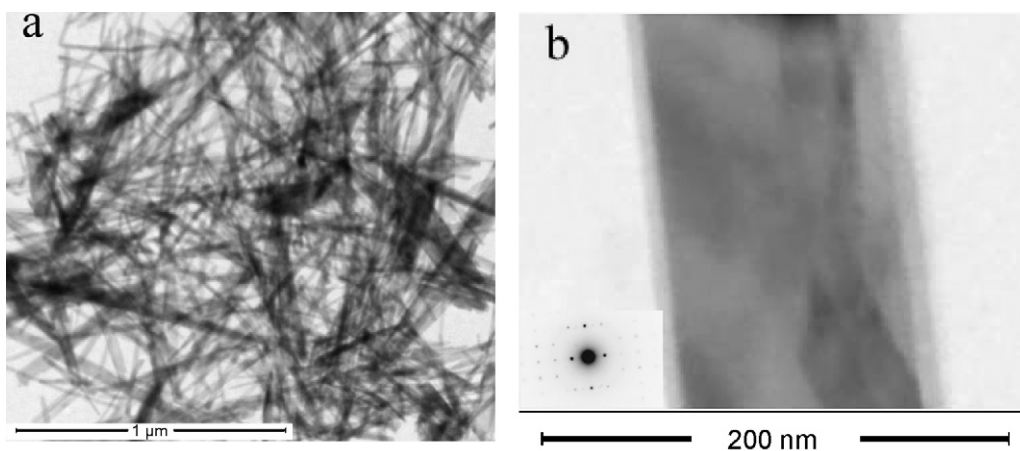


Fig. 4. TEM of the prepared hydrophobic zinc borate with phosphate ester at 70 °C and pH 8 for 7 h: (a) low-magnification image and (b) high-magnification image (inset the SAED).

(Fig. 6a), with phosphate ester (Fig. 6b) and the pure phosphate ester had different frameworks. There were CH_2 bands at 910 and 1400 cm^{-1} , P–O–C band at 1003 cm^{-1} , and PO_2 asymmetric stretching band at 1329 cm^{-1} (Fig. 6b). So the phosphate ester was bonded to the surface of zinc borate.

3.7. SEM micrograph of the polymers

Many properties of materials would be affected by their morphology. Fig. 7 shows the comparable SEM micrographs of the fractured surface of PE without (Fig. 7a) and with h-ZB

(Fig. 7b). A number of discontinuous blocks had created large voids, which was unexpected in the macromolecule materials (Fig. 7a). On the other hand, the micrograph of composite PE after compounding with 50% (w/w) the hydrophobic zinc borate (Fig. 7b) illustrated that the fracture surface appeared to be homogeneous and continuous. There were no obvious blocks of PE observed. Furthermore, the interface was not clear and the gaps in the polymers had disappeared. This improved interfacial adhesion might be caused by the compatible effect of composite, which could be explained by the hydrophobicity of zinc borate.

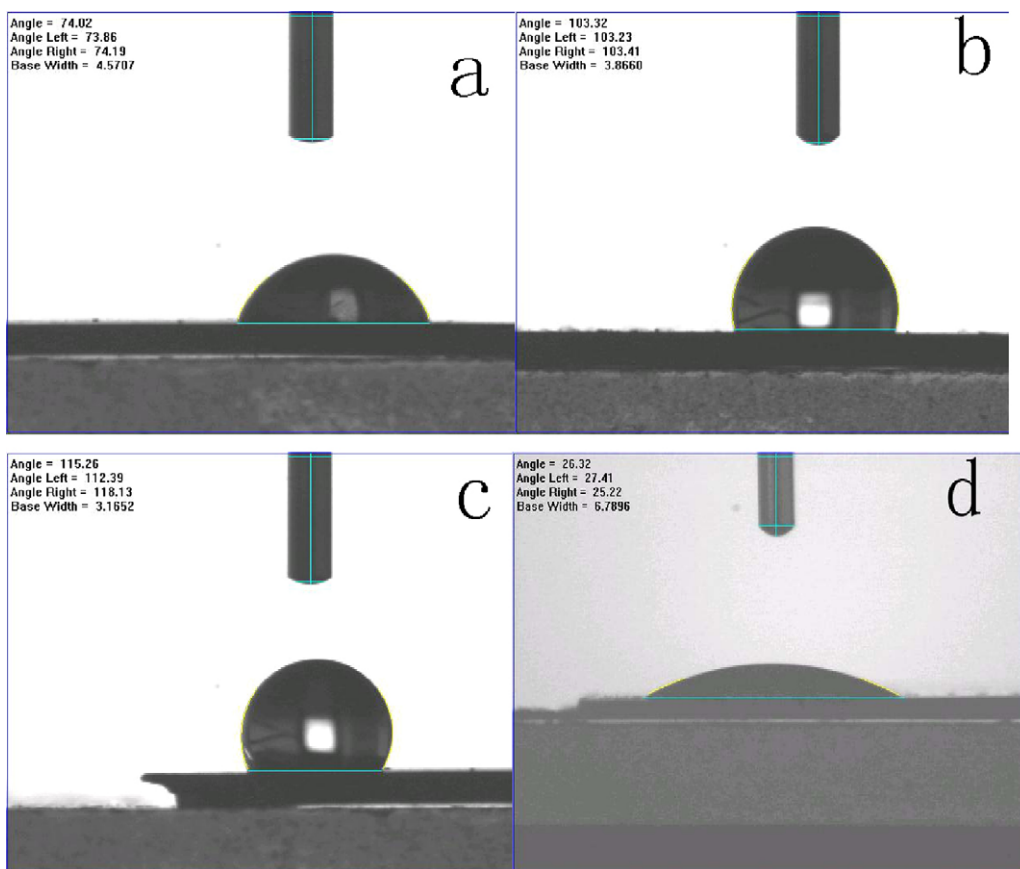


Fig. 5. Contact angle of samples prepared at pH 8 for 7 h: (a) at 30 °C with phosphate ester; (b) at 50 °C with phosphate ester; (c) at 70 °C with phosphate ester; (d) at 70 °C without phosphate ester.

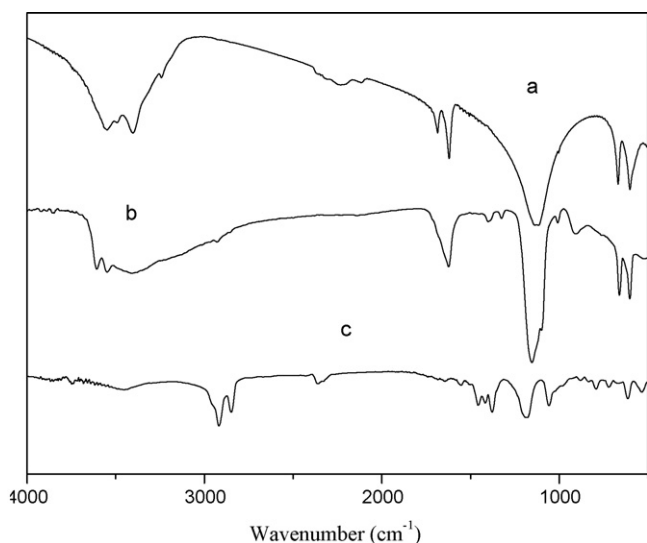


Fig. 6. FT-IR spectra of the powders were prepared at 70 °C and pH 8 for 7 h: (a) without phosphate ester; (b) with phosphate ester; (c) pure phosphate ester.

3.8. Thermogravimetric analysis of the composites

TGA is widely used to investigate the thermal decomposition of polymers and to determine the kinetic parameters such as activation energy and order of reaction. These parameters can be used to give a better understanding of the thermal stability of polymer blends.

The thermal stabilities of the h-ZB/PE with different amounts of the hydrophobic zinc borate added in PE are compared with that of the pure PE in Fig. 8, respectively. The thermal stabilities of h-ZB/PE nanocomposites were improved with the addition of h-ZB as the thermal stabilities of pure PE which were lower than the h-ZB/PE composites (Fig. 8).

Fig. 9 summarizes the percentage weight loss at different addition of h-ZB in PE at 600 °C taken from the TGA thermograms (Fig. 8). It could be seen that (from the thermograms) h-ZB/PE composites lost about 67% of the total weight at 422 °C at addition of 50% h-ZB in PE.

Fig. 10 summarizes the degraded temperature at different addition of h-ZB/PE taken from the TGA thermograms (Fig. 8). It could be seen that the degraded temperature of h-ZB/PE polymers had been 420 °C when the accretion reached 47%. And then, the degraded temperature had not presented biggish changes along with the

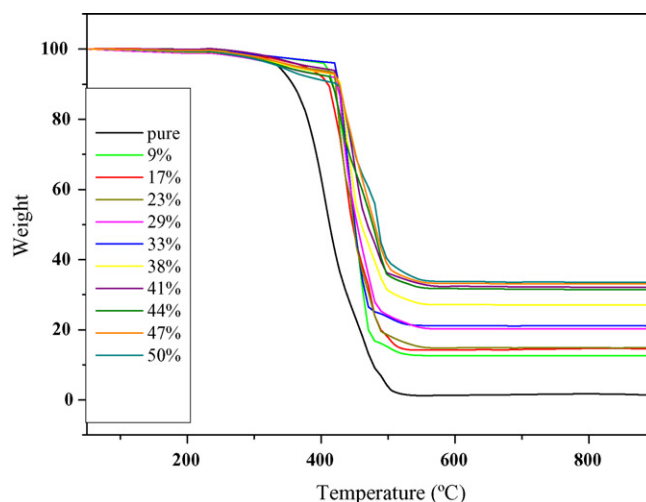


Fig. 8. TGA of PE with various amount of the hydrophobic zinc borate (h-ZB).

increasing percentage of h-ZB. The results showed that the addition of the nanowhiskers could improve the degraded temperature of organic polymers (PE) from 317 to 422 °C. It indicated that the addition of the h-ZB nanowhiskers had improved the thermal stabilities of the organic polymers.

3.9. The mechanism of synthesis

In principle, crystal growth and crystal morphology are governed by extrinsic and intrinsic factors, including the degree of supersaturation, the diffusion of the reaction, the surface and interfacial energy, and the structure of the crystals. On the basis of experimental data obtained previously, there are at least three factors that are responsible for the shape and size of the $4\text{ZnO}\cdot\text{B}_2\text{O}_3\cdot\text{H}_2\text{O}$ crystals. The first is the surfactant phosphate ester, which plays an important role in the present synthesis of hydrophobic zinc borate nanowhiskers. In a parallel experiment, if no phosphate ester was added into the reaction mixture, nanowhiskers would not be obtained (Fig. 3a). Phosphate ester and metal ions formed a strong electrovalent bond with the raise of reaction temperature, resulting in modified products with hydrophobic properties.

According to the Gibbs–Curie–Wulff theorem, the growth rates on different surface facets are dominated by the surface energy. When a particle grows, the facets tend toward low-energy planes to minimize the surface energy. The $4\text{ZnO}\cdot\text{B}_2\text{O}_3\cdot\text{H}_2\text{O}$ crystals nucle-

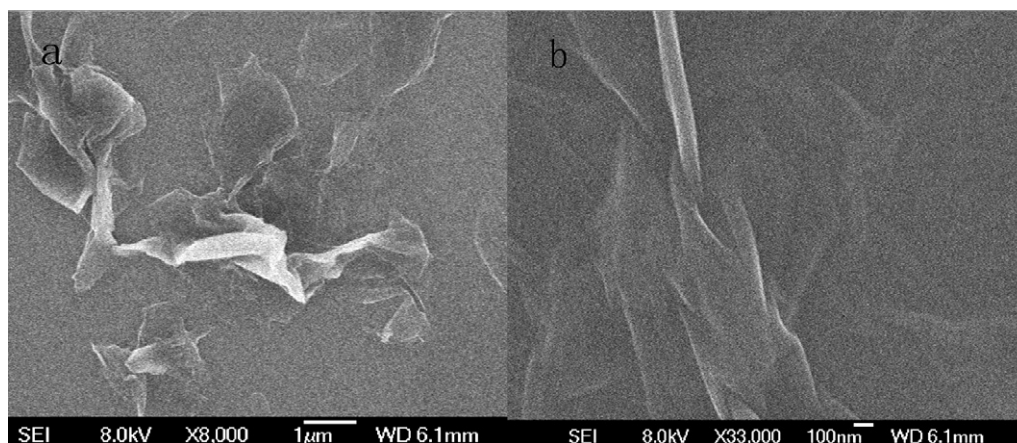


Fig. 7. SEM images of samples: (a) pure PE and (b) h-ZB/PE.

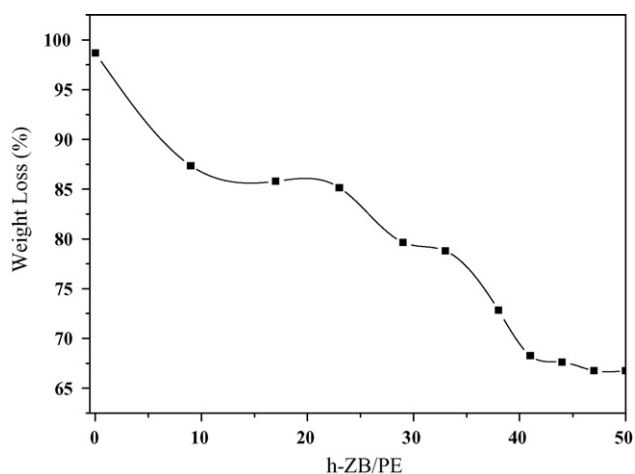


Fig. 9. Influence of the amount of the hydrophobic zinc borate (h-ZB) on the weight loss of PE.

ate and grow on the surface of the Zn–phosphate ester complexing template. The intrinsic crystal growth is modulated extrinsically by phosphate ester adsorption on certain crystallographic facets that inhibit the growth of some crystal planes and results in different growth rates during particle growth, thus tailoring the crystal shapes. Finally, the modified products were hydrophobic.

The other two factors are the reaction temperature and pH. When the reaction temperature was increased to 70 °C, the mode of phosphate ester chains and crystal growth were affected. On the basis of the previous work and our experimental observation, phosphate ester in the present synthetic method was to generate large numbers of whiskerlike micelle in aqueous solution, which might act as soft-templates for the formation of 1D nanostructures. In addition, the temperature would significantly influence the aggregation state of surfactant in solution. From Fig. 3b–d, the number of zinc borate whiskers apparently increased with the increasing temperature, which might be explained that the reaction had been a kinetic-driven process at higher temperatures. Thus, these hydrophobic zinc borate nanowhiskers crystals were the only product when the temperature reached 70 °C (Fig. 3e).

As to pH, the infection could be explained using the following three equations:

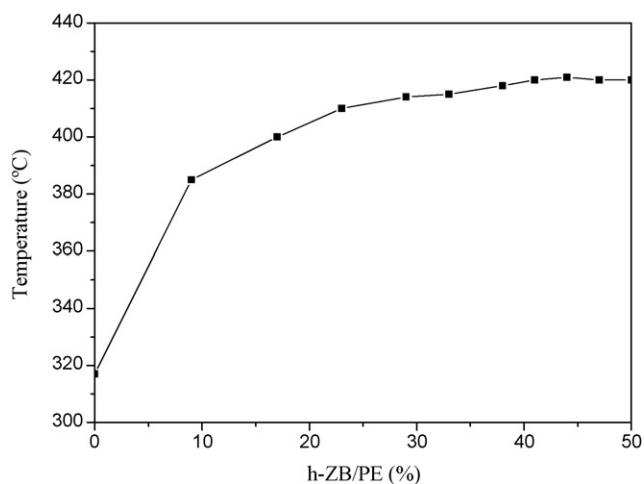
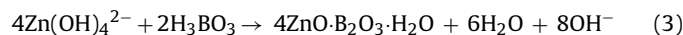


Fig. 10. Influence of the amount of the hydrophobic zinc borate (h-ZB) on the thermal stability of PE.



The nanowhiskers could not be obtained at a pH other than 8. These experiment results indicated that the starting pH of the current reaction system had a significant role in the formation of the final products. The initial pH controlled the speciation of ions, with $\text{Zn}(\text{OH})_4^{2-}$ being significantly affected, whereas the existing amount of $\text{Zn}(\text{OH})_4^{2-}$ was crucial for the fabrication of $4\text{ZnO} \cdot \text{B}_2\text{O}_3 \cdot \text{H}_2\text{O}$. At lower pH, OH^- was insufficient and could not promote the equilibrium reaction (2) to the right, resulting in the unavailability of $\text{Zn}(\text{OH})_4^{2-}$ in the reaction system, and therefore, $4\text{ZnO} \cdot \text{B}_2\text{O}_3 \cdot \text{H}_2\text{O}$ could not be formed. When the higher pH existed in the reaction system, the chemical equilibrium 2 shifted to the right, and $4\text{ZnO} \cdot \text{B}_2\text{O}_3 \cdot \text{H}_2\text{O}$ was intended to be formed. When an excess of OH^- existed in the solution ($\text{pH} > 8$), the chemical equation 1 shifted to the left, and there was not enough H_3BO_3 to be used to form the $4\text{ZnO} \cdot \text{B}_2\text{O}_3 \cdot \text{H}_2\text{O}$ in equilibrium 3.

3.10. The mechanism of performance

The interface of polymers was not clear, and there were many gaps in the polymers. The interstices had disappeared with the addition of inorganic particles. The interfacial adhesion improved and then the compatible of polymer could be enhanced, which could be explained by the addition of h-ZB. The h-ZB could disperse in the polymers better than the other unmodified inorganic particles. The h-ZB spread around the polymers to fill up the interspaces and then improved their thermal stability.

Furthermore, the presence of the nanoparticles filler led to prodigious changes in thermogram. In particular, the degradation temperatures of both h-ZB and PE were increased at small weight loss values. These results confirmed quantitatively that at weight loss values lower than 20% the nanoparticles were able to increase PE thermal stability.

The weight loss step occurred from 400 to 600 °C and reflected the occurrence of thermal-oxidative degradation of the char. This process was slowed down for h-ZB nanocomposites, suggesting an increased stability. Moreover, the partially desquamated nanocomposite showed an increase in the temperature of the maximum decomposition rate, indicating improved stabilization against the oxidative process with respect to the intercalated composite. It was reasonable to hypothesize that the presence of the nanoparticles retarded the thermal transfer, and hindered the oxygen diffusion into the polymer bulk.

In the curves (Fig. 8), the weight loss had not increased along with the addition of the h-ZB. The reason may be described that the h-ZB/PE had been saturated when the amount of h-ZB reaches 41%, and then, some assembled nanoparticles had prevented the weight of h-ZB/PE lost.

4. Conclusions

$4\text{ZnO} \cdot \text{B}_2\text{O}_3 \cdot \text{H}_2\text{O}$ nanowhiskers were successfully obtained by $\text{Na}_2\text{B}_4\text{O}_7 \cdot 10\text{H}_2\text{O}$ and $\text{Zn}(\text{NO}_3)_2 \cdot 6\text{H}_2\text{O}$ as raw materials via one-step precipitation reaction, and phosphate ester as the soft template. XRD analysis indicated that the product was highly pure and monoclinic. SEM analysis indicated that the morphology of products only displayed nanowhiskers with diameters of 50–100 nm, lengths of about 1 μm, and the aspect ratios of 10–20. The products were well dispersed into polyethylene. These results demonstrated that the presence of phosphate ester and the change of temperature were crucial for the preparation of zinc borate nanowhiskers, consistent with the suggested formation mechanism.

References

- [1] S.Y. Fu, B. Lauke, E. Maèder, X. Hu, C.Y. Yue, Tensile properties of short-glass-fiber- and short-carbon-fiber-reinforced polypropylene composites, *Compos. Part A* 31 (2000) 1117–1125.
- [2] S.A. Gordeyev, J.A. Ferreira, C.A. Bernardo, I.M. Ward, A promising conductive material: highly oriented polypropylene filled with short vapour-grown carbon fibres, *Mater. Lett.* 51 (2001) 32–36.
- [3] R.J. Kuriger, M.A. Khairul, P.D. Anderson, R.L. Jacobson, Processing and characterization of aligned vapor grown carbon fiber reinforced polypropylene, *Compos. Part A* 33 (2002) 53–62.
- [4] M. Grunert, T.W. Winter, Nanocomposites of cellulose acetate butyrate reinforced with cellulose nanocrystals, *J. Polym. Environ.* 10 (2002) 27–30.
- [5] K. Tashiro, M. Kobayashi, Theoretical evaluation of three-dimensional elastic constants of native and regenerated celluloses: role of hydrogen bonds, *Polymer* 32 (1991) 1516–1526.
- [6] R. Ma, Y. Bando, T. Sato, C. Tang, F. Xu, Single-crystal $\text{Al}_{18}\text{B}_4\text{O}_{33}$ microtubes, *J. Am. Chem. Soc.* 124 (2002) 10668–10669.
- [7] Y. Kong, F.S. Li, Cohesive energy, local magnetic properties, and Curie temperature of Fe_3B studied using the self-consistent LMTO method, *Phys. Rev. B* 56 (1997) 3153–3158.
- [8] M. Morkoc, S.N. Mohammad, High-luminosity blue and blue-green gallium nitride light-emitting diodes, *Science* 267 (1995) 51–55.
- [9] C. Kane, L. Balents, M.P.A. Fisher, Coulomb interactions and mesoscopic effects in carbon nanotubes, *Phys. Rev. Lett.* 79 (1998) 5086–5089.
- [10] A. Bansal, H. Yang, C. Li, B.C. Benicewicz, S.K. Kumar, L.S. Schadler, Controlling the thermomechanical properties of polymer nanocomposites by tailoring the polymer–particle interface, *J. Polym. Sci. Polym. Phys.* 44 (2006) 2944–2950.
- [11] J. Xu, F. Qiu, H.Y. Zhang, Morphology and interactions of polymer brush-coated spheres in a polymer matrix, *J. Polym. Sci. Polym. Phys.* 44 (2006) 2811–2820.
- [12] S.S. Lee, J. Kim, Surface modification of clay and its effect on the intercalation behavior of the polymer/clay nanocomposites, *J. Polym. Sci. Polym. Phys.* 42 (2004) 2367–2372.
- [13] D. Ciprai, K. Jacob, R. Tannenbaum, Characterization of polymer nanocomposite interphase and its impact on mechanical properties, *Macromolecules* 39 (2006) 6565–6573.
- [14] L. Schadler, Nanocomposites: model interfaces, *Nat. Mater.* 6 (2007) 257–258.
- [15] P. Rittiqstein, J.M. Torkelson, Polymer–nanoparticle interfacial interactions in polymer nanocomposites: confinement effects on glass transition temperature and suppression of physical aging, *J. Polym. Sci. Polym. Phys.* 44 (2006) 2935–2943.
- [16] M.A.S. Azizi Samir, F. Alloin, A. Dufresne, Review of recent research into cellulosic whiskers, their properties and their application in nanocomposite field, *Biomacromolecules* 6 (2005) 612–626.
- [17] J.J. Urban, W.S. Yun, Q. Gu, H. Park, Synthesis of single-crystalline perovskite nanorods composed of barium titanate and strontium titanate, *J. Am. Chem. Soc.* 124 (2002) 1186–1187.
- [18] Y.M. Tian, Y.P. Guo, M. Jjiang, Y. Sheng, B.L. Hari, G.Y. Zhang, Y.Q. Jjiang, B. Zhou, Y.C. Zhu, Z.C. Wang, Synthesis of hydrophobic zinc borate nanodiscs for lubrication, *Mater. Lett.* 60 (2006) 2511–2515.
- [19] Y.M. Tian, Y. He, L.X. Yu, Y.H. Deng, Y.H. Zheng, F. Sun, Z.H. Liu, Z.C. Wang, In situ and one-step synthesis of hydrophobic zinc borate nanoplatelets, *Coll. Surf. A: Physicochem. Eng. Aspects* 312 (2008) 99–103.
- [20] X.X. Shi, L.J. Yuan, X.Z. Sun, C.X. Chang, J.Y. Sun, Controllable synthesis of $4\text{ZnO}\cdot\text{B}_2\text{O}_3\cdot\text{H}_2\text{O}$ nano-/microstructures with different morphologies: influence of hydrothermal reaction parameters and formation mechanism, *J. Phys. Chem. C* 112 (2008) 3558–3567.
- [21] G. Corbel, E. Suard, J. Emery, M. Leblanc, OH–F disorder in non-centrosymmetric $\text{Zn}_2(\text{BO}_3)(\text{OH})_{0.75}\text{F}_{0.25}$: ab initio structure determination and NMR study; comparison with tridymite and fluoride borates, *J. Alloys Compd.* 305 (2000) 49–57.